CrossMark

ORIGINAL PAPER

Study on factors governing the conductivity performance of acylated chitosan-NaI electrolyte system

F.H. Muhammad[1] · Asheila Jamal[2] · Tan Winie[2]

Abstract Hexanoyl chitosan and lauroyl chitosan were prepared by acyl modification of chitosan. Films of hexanoyl chitosan- and lauroyl chitosan-based polymer electrolytes incorporated with different weight concentrations of sodium iodide (NaI) were prepared using the solution casting technique. FTIR and differential scanning calorimetry (DSC) results suggested that NaI interacted with both hexanoyl chitosan and lauroyl chitosan. Maximum conductivities of 1.3×10^{-6} and 1.1×10^{-8} S cm^{-1} are achieved for hexanoyl chitosan and lauroyl chitosan, respectively. Higher conductivity in hexanoyl chitosan is attributed to higher ion mobility as supported by DSC results. The dielectric constants of neat hexanoyl chitosan and lauroyl chitosan are 2.7 and 1.9, respectively, estimated from impedance spectroscopy. Higher dielectric constant of hexanoyl chitosan resulted in greater NaI dissociation and hence higher conductivity. Deconvolution of O=C-NHR and OCOR bands of polymer has been carried out to estimate the amount of dissociated Na$^+$ ions from NaI. The findings were in good agreement with conductivity results. In order to assess quantitatively, the conductivity, parameter number, n, and mobility, μ, of ions were calculated using impedance spectroscopy. XRD results showed the influence of NaI on the crystalline content of the electrolyte system. Sample with lower crystalline content exhibited higher conductivity.

Introduction

Natural polymer is an attractive option in solid polymer electrolytes (SPEs) owing to their abundant sources, low cost, and nontoxicity. Natural polymers such as chitosan, starch, cellulose, gellan gum, and carrageenan are alternative host for SPE [1–4]. Among these natural polymers, chitosan is under extensive research [5, 6]. Chitosan is a linear copolymer of β-(1–4)-linked glucosamine and *N*-acetyl-glucosamine, obtained by *N*-deacetylation of chitin. Presence of lone pair electrons at the hydroxyl and amine groups of chitosan allows complexation between chitosan and the doping salt.

However, the rigid crystalline structure of chitosan and its poor solubility in large number of solvents limit its utilization. In order to improve the solubility of chitosan, chemical modification such as acyl modification [7, 8], phthaloylation [9], and alkylation [10] of chitosan has been carried out. Zong et al. [8] have reported on the acyl modification of chitosan reacted with hexanoyl and lauroyl chlorides. The hexanoyl and lauroyl substituted chitosans were known as hexanoyl and lauroyl chitosan, respectively. Our previous works on SPEs focused on hexanoyl chitosan. Conductivity as high as ~10^{-4} S cm^{-1} could be achieved for hexanoyl chitosan-LiCF$_3$SO$_3$/PC/EC electrolyte system [11]. However, plasticizer affected the mechanical strength

✉ Tan Winie
tanwinie@salam.uitm.edu.my

1 Center of Foundation Studies, Universiti Teknologi MARA, 43800 Dengkil, Selangor, Malaysia

2 Faculty of Applied Sciences, Universiti Teknologi MARA, 40450 Shah Alam, Selangor, Malaysia

of hexanoyl chitosan. Blending hexanoyl chitosan with polystyrene achieved a combination of good conductivity and mechanical stability. The increased conductivity in the blends is achieved by decreasing the crystallinity fraction of hexanoyl chitosan and by controlled percolation of Li salt in hexanoyl chitosan phase when polystyrene is added to hexanoyl chitosan [12–14]. Presence of TiO$_2$ fillers further improved the conductivity and mechanical properties of hexanoyl chitosan/polystyrene blends [15]. Up to date, there is no report on lauroyl chitosan-based SPEs published in the literature. The hexanoyl chitosan and lauryl chitosan have different characteristics as shown in Table 1. Thus, in this work, we would like to adopt hexanoyl chitosan and lauroyl chitosan as the host matrix and compare their conductivity performance. Sodium iodide (NaI) was employed as the doping salt due to its availability in abundance, low cost, and less reactivity compared to lithium salt. This paper began with the investigation of the hexanoyl chitosan-NaI and lauroyl chitosan-NaI interactions by FTIR and differential scanning calorimetry (DSC), followed by the conductivity performance of hexanoyl chitosan- and lauroyl chitosan-based SPEs. In order to analyze quantitatively the conductivity trend observed, parameters such as number and mobility of ions were calculated using impedance spectroscopy.
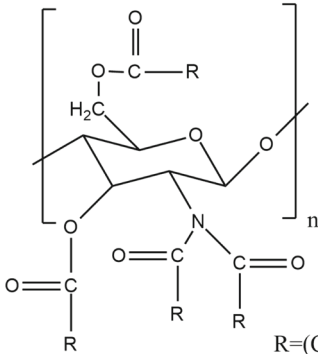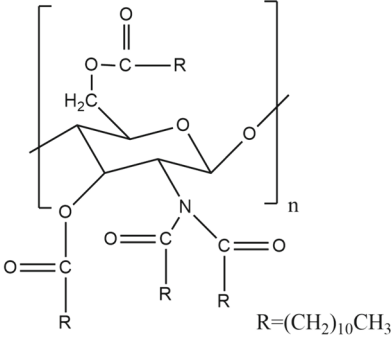
Experimental

Sample preparation

Hexanoyl chitosan and lauroyl chitosan that exhibited solubility in tetrahydrofuran (THF) were prepared in a similar manner as previously described in [8]. Chitosan with molecular weight, M_w, of 6.0×10^5 g mol^{-1} from Aldrich was used as received. Figure 1 shows the reaction scheme in forming hexanoyl chitosan and lauroyl chitosan from chitosan. The characteristics of the two polymers are given in Table 1.

NaI with purity 99% from Aldrich was used as received. The salted hexanoyl chitosan and lauroyl chitosan systems were prepared by dissolving the required amount of hexanoyl chitosan and/or lauroyl chitosan with different amounts of NaI ranging from 5 to 40 wt% separately in THF. The solutions were mixed and stirred at room temperature for over 24 h until complete dissolution. The solutions were then cast in Teflon petri dishes and allowed to evaporate at room temperature until films were formed. The films were kept in a dessicator for continuous drying.

Sample characterization

Thermal analyses were performed using DSC instrument (TA Q200). The samples were heated from −90 to 100 °C at a

Table 1 Characteristics of hexanoyl chitosan and lauroyl chitosan

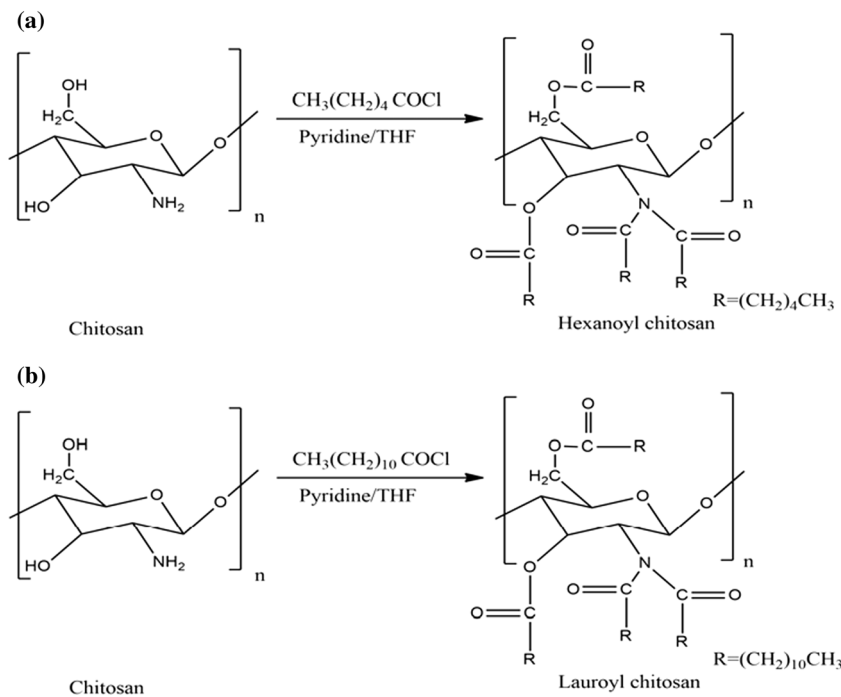| Polymer	Hexanoyl chitosan	Lauroyl chitosan
$M_w{}^a$ / g mol^{-1}	8.7×10^5	3.0×10^6
$T_g{}^b$ / °C	-24.0	-10.0
$\varepsilon_r{}^c$	2.7	1.9
Molecular structure		

R=(CH$_2$)$_4$CH$_3$ R=(CH$_2$)$_{10}$CH$_3$

[a] Weight average of molecular weight as estimated in this work by Waters Gel Permeation Chromatography (GPC). Polystyrene with low polydispersity was used as standard

[b] Glass transition temperature by differential scanning calorimetry as determined in this work

[c] Dielectric constant by impedance analyzer as determined in this work

Fig. 1 Formation of **a** hexanoyl chitosan and **b** lauroyl chitosan from chitosan

(a)

Chitosan → Hexanoyl chitosan

CH$_3$(CH$_2$)$_4$COCl
Pyridine/THF

R=(CH$_2$)$_4$CH$_3$

(b)

Chitosan → Lauroyl chitosan

CH$_3$(CH$_2$)$_{10}$COCl
Pyridine/THF

R=(CH$_2$)$_{10}$CH$_3$

heating rate of 10 °C/min (isothermal hold for 5 min), followed by quenching cool to −90 °C at 10 °C/min for 5 min. The samples were then heated up to 100 °C at a heating rate of 10 °C/min under dry nitrogen. The glass transition temperatures, T_g, were determined from the second heating scan.

ATR-FTIR spectra were recorded using a FTIR-iS10 Nicolet spectrophotometer in the frequency range from 600 to 4000 cm^{-1} at a resolution of 2 cm^{-1}. The spectral features obtained were analyzed and fitted with a Gaussian/Lorentzian function using the Origin 8.0 software.

XRD studies were carried out using X-Pert PRO XRD. The samples were directly scanned at 2θ angles between 5° and 80°. The X-ray source used was CuKα with a wavelength of 1.5418 Å.

Impedance measurements of the films were carried out using HIOKI 3532-50 LCR Hi Tester in the frequency range of 50 Hz to 1 MHz. The prepared sample film was sandwiched between two stainless steel electrodes with diameter 1.2 cm under spring pressure. The ionic conductivity, σ, of the sample was calculated using the following equation:

$$\sigma = \frac{t}{RA} \quad (1)$$

where t is the thickness of the film and A is the film-electrode contact area. The bulk resistance, R, was determined from the complex impedance plot with the horizontal and vertical axes having the same scale. The ionic conductivity is described by

$$\sigma = en\mu \quad (2)$$

where e is the electronic charge, n is the number density of free ions, and μ is the ion mobility.

Complex impedance plots obtained in this work take the form of a depressed semicircle and a tilted spike. This can be represented by an equivalent circuit that consists of parallel combination of a resistor and a constant phase element (CPE) [16] connected in series with another CPE as shown in Fig. 2.
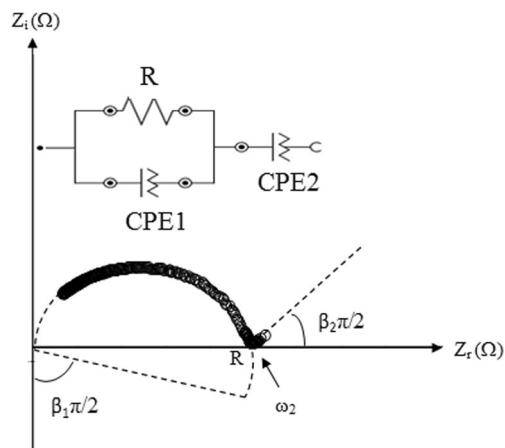

Fig. 2 Complex impedance plot for parallel combination of a resistor and a CPE that are connected in series with another CPE

The impedance, Z_1, for the parallel combination of a resistor and CPE is given as

$$\frac{1}{Z_1} = \frac{1}{R} + \frac{1}{Z_{CPE1}} \qquad (3)$$

where the impedance of CPE is

$$Z_{CPE} = \frac{1}{Q\omega^\beta}\cos\left(\frac{\beta\pi}{2}\right) - j\frac{1}{Q\omega^\beta}\sin\left(\frac{\beta\pi}{2}\right) \qquad (4)$$

with Q is the capacitance of a CPE [17].

Substituting Eq. (4) to Eq. (3), the impedance Z_1 is read as

$$\frac{1}{Z_1} = \frac{1}{R} + \frac{1}{\dfrac{1}{Q_1\omega^{\beta_1}}\cos\left(\frac{\beta_1\pi}{2}\right) - j\dfrac{1}{Q_1\omega^{\beta_1}}\sin\left(\frac{\beta_1\pi}{2}\right)} \qquad (5)$$

which leads to

$$Z_1 = \frac{1}{\left[\dfrac{1}{R} + Q_1\omega^{\beta_1}\cos\left(\frac{\beta_1\pi}{2}\right)\right] + j\left[Q_1\omega^{\beta_1}\sin\left(\frac{\beta_1\pi}{2}\right)\right]} \qquad (6)$$

The total impedance, Z_{tot}, after inclusion of the second CPE component as shown in Fig. 2 is given as

$$Z_{tot} = Z_1 + Z_{CPE2} \qquad (7)$$

Substituting Eqs. (4) and (6) to Eq. (7), it follows that

$$Z_{tot} = \frac{1}{\left[\frac{1}{R} + Q_1\omega^{\beta_1}\cos\left(\frac{\beta_1\pi}{2}\right)\right] + j\left[Q_1\omega^{\beta_1}\sin\left(\frac{\beta_1\pi}{2}\right)\right]} + \frac{1}{Q_2\omega^{\beta_2}}\cos\left(\frac{\beta_2\pi}{2}\right) - j\frac{1}{Q_2\omega^{\beta_2}}\sin\left(\frac{\beta_2\pi}{2}\right) \qquad (8)$$

Hence, the real, Z_r, and imaginary, Z_i, parts of the Z_{tot} are given by

$$Z_r = \frac{\frac{1}{R} + Q_1\omega^{\beta_1}\cos\left(\frac{\beta_1\pi}{2}\right)}{\left[\frac{1}{R} + Q_1\omega^{\beta_1}\cos\left(\frac{\beta_1\pi}{2}\right)\right]^2 + \left[Q_1\omega^{\beta_1}\sin\left(\frac{\beta_1\pi}{2}\right)\right]^2}$$
$$+ \frac{1}{Q_1\omega^{\beta_2}}\cos\left(\frac{\beta_1\pi}{2}\right) \qquad (9)$$

and

$$Z_i = \frac{Q_1\omega^{\beta_1}\sin\left(\frac{\beta_1\pi}{2}\right)}{\left[\frac{1}{R} + Q_1\omega^{\beta_1}\cos\left(\frac{\beta_1\pi}{2}\right)\right]^2 + \left[Q_1\omega^{\beta_1}\sin\left(\frac{\beta_1\pi}{2}\right)\right]^2}$$
$$+ \frac{1}{Q_2\omega^{\beta_2}}\sin\left(\frac{\beta_2\pi}{2}\right) \qquad (10)$$
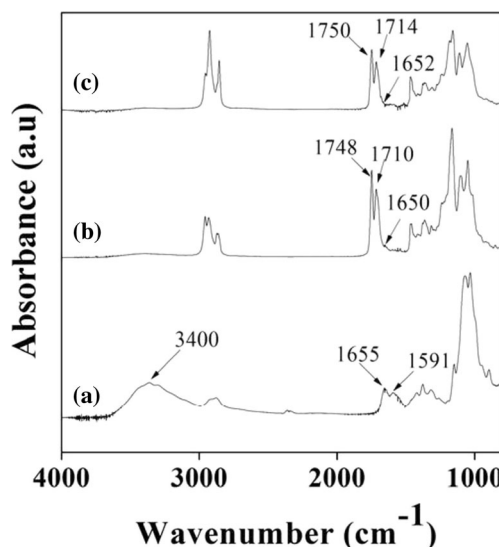

Fig. 3 Infrared spectra between 700 and 4000 cm^{-1} for a chitosan, b hexanoyl chitosan, and c lauroyl chitosan

where R is the bulk resistance of the electrolyte, Q_1 is the bulk capacitance of the electrolyte, and Q_2 is the capacitance due to the double layer formed at the electrolyte-electrode interface. Equations (9) and (10) are used to fit the complex impedance plots to obtain the values of R, Q_1, Q_2, β_1, and β_2.

According to Arof and coworkers [18], the diffusion coefficient, D, of charge carriers developed from complex impedance plot is

$$D = \frac{1}{\tau_2}\left(\frac{\varepsilon_r\varepsilon_o A}{Q_2}\right)^2 \qquad (11)$$

where ε_o is the permittivity of free space and A is the electrolyte-electrode contact area. ε_r is the dielectric constant of the electrolyte that can be obtained from the log ε_r vs.

Table 2 IR peaks for hexanoyl chitosan and lauroyl chitosan incorporated with different NaI concentrations at room temperature

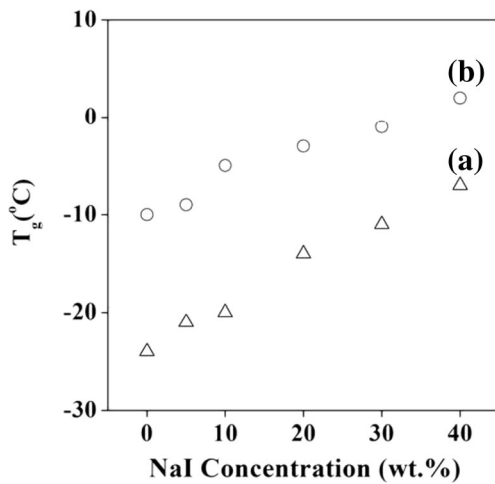| NaI content (wt%)	Vibrational mode (cm^{-1})		
	N(COR)$_2$	OCOR	O=C-NHR
(a) Hexanoyl chitosan-NaI system			
0	1748	1710	1650
10	1746	1713	1641
20	1746	1715	1638
30	1745	1715	1625
40	1743	1716	1622
(b) Lauroyl chitosan-NaI system			
0	1750	1714	1652
10	1749	1715	1630
20	1749	1716	1625
30	1747	1716	1624
40	1746	1717	1620

Fig. 4 Variation of T_g with NaI content for *a* salted hexanoyl chitosan and *b* salted lauroyl chitosan electrolyte system

frequency plot. τ_2 is $1/\omega_2$ with ω_2 being the minimum angular frequency in the Z_i (see Fig. 2) [14, 18]. The value of Q_2 was obtained by trial and error until Eqs. (9) and (10) fit the complex impedance plot. Thus, knowing D, the mobility, μ, of free ions can be determined in accordance with the Nernst-Einstein equation

$$\mu = \frac{eD}{k_B T} \tag{12}$$

Substituting μ in Eq. (2) with Eq. (12), the number of free ions, n can be described as

$$n = \frac{\sigma k_B T}{e^2 D} \tag{13}$$

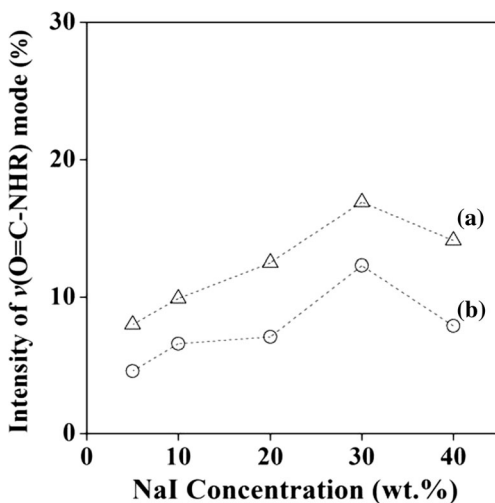where k_B is the Boltzmann constant, T is the absolute temperature in Kelvin, and e has its usual meaning.

Fig. 5 Intensity of ν(O=C-NHR) mode for *a* hexanoyl chitosan and *b* lauroyl chitosan electrolyte systems with respect to the NaI concentration
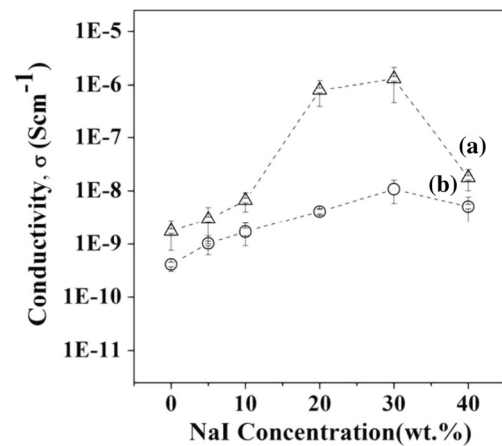

Fig. 6 Room temperature conductivity for *a* salted hexanoyl chitosan and *b* salted lauroyl chitosan system

Results and discussion

Hexanoyl chitosan-NaI and lauroyl chitosan-NaI interaction

Figure 3 presents the infrared spectra of chitosan, hexanoyl chitosan and lauroyl chitosan in the region between 700 and 4000 cm^{-1}. The carboxamide, O=C-NHR band of chitosan at 1655 cm^{-1} appeared as a small shoulder in hexanoyl chitosan at 1650 cm^{-1} and in lauroyl chitosan at 1652 cm^{-1}. The amine, NH$_2$ band of chitosan at 1591 cm^{-1}, was absent in both hexanoyl chitosan and lauroyl chitosan, indicating that the amino group of chitosan had converted to amide group.

In the spectrum of hexanoyl chitosan and lauroyl chitosan, two new peaks of O=C of N(COR)$_2$ and OCOR were observed. For hexanoyl chitosan, peaks of O=C of N(COR)$_2$ and OCOR were observed at 1748 and 1710 cm^{-1}, respectively. For lauroyl chitosan, the peaks were observed at 1750 and 1714 cm^{-1}, respectively. These peaks were not present in the chitosan spectrum.
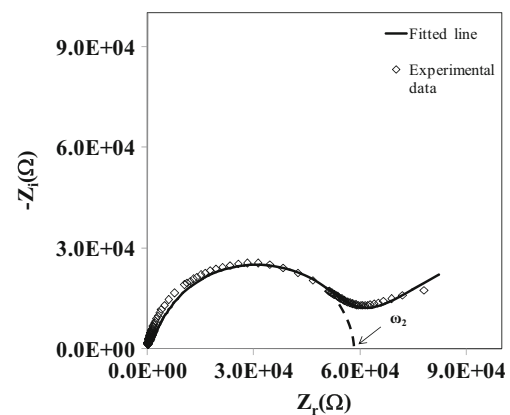

Fig. 7 Complex impedance plot of hexanoyl chitosan with 30 wt% NaI at room temperature. *Diamonds* experimental data and *dashed line* fitted line
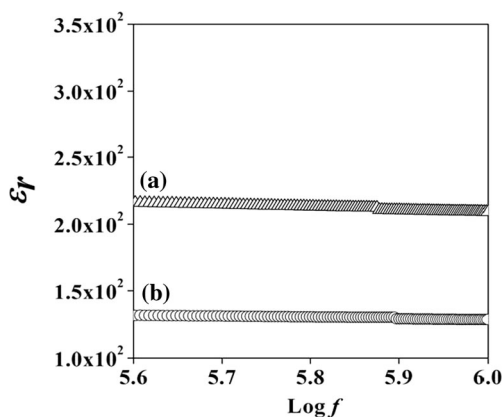
Fig. 8 Room temperature ε_r vs. log f plot for *a* hexanoyl chitosan-30 wt% NaI and *b* lauroyl chitosan-30 wt% NaI

Fig. 9 Room temperature ε_r vs. log f plot for *a* neat hexanoyl chitosan and *b* neat lauroyl chitosan

A broad OH-stretching band centered at 3400 cm^{-1} was observed in chitosan spectrum but disappeared in the spectrum of hexanoyl chitosan and lauroyl chitosan, indicating that the OH and CH$_2$OH in the structure of chitosan were acylated.

Table 2 presents the IR peaks for hexanoyl chitosan and lauroyl chitosan incorporated with different concentrations of NaI. Addition of NaI shifted the position of the NCOR$_2$, OCOR, and O=C-NHR bands. This implied that Na$^+$ ions from the salt had formed complexation with donor atoms of hexanoyl chitosan and lauroyl chitosan.

The formation of hexanoyl chitosan-NaI and lauroyl chitosan-NaI complexes was further supported by the results from DSC as demonstrated in Fig. 4. The glass transition temperature, T_g, for neat hexanoyl chitosan and neat lauroyl chitosan was detected at −24 and −10 °C, respectively. It was found that T_gs for both hexanoyl chitosan and lauroyl chitosan increased with increasing NaI concentration. Na$^+$ ions interacted with the donor atoms of hexanoyl chitosan and lauroyl chitosan via transient cross-linking interactions. These interactions reduced the segmental movement of polymer chains. In other words, the flexibility of polymer backbone was reduced and this was reflected by an increase in T_gs for the polymer-salt complexes.

Sim et al. [19] reported that Li$^+$ cations interact with the oxygen atom in O=C of poly(ethyl methacrylate) (PEMA), and thus, the intensity of ν(C=O) can be used to indicate the amount of Li$^+$ ions that have complexed with O=C of PEMA. Similarly, the amount of Na$^+$ cations that have complexed with the oxygen atom in O=C-NHR of hexanoyl chitosan
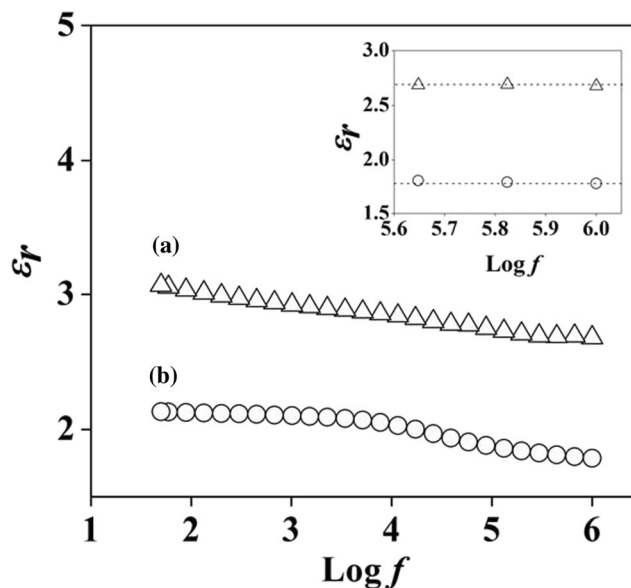
(or lauroyl chitosan) is reflected in the intensity of ν(O=C-NHR). Deconvolution of ν(O=C-NHR) mode has been carried out to estimate the number of Na$^+$ ions coordinated on O=C-NHR functional group. Figure 5 shows the plot of the intensity of ν(O=C-NHR) mode with respect to various NaI concentrations for salted hexanoyl chitosan and lauroyl chitosan systems. It was observed that for both hexanoyl chitosan and lauroyl chitosan electrolytes, the intensity of O=C-NHR band increased with increasing concentration of NaI up to 30 wt%. In other words, the number of dissociated Na$^+$ ions from NaI increases with increasing NaI concentration and reaches a maximum at 30 wt%. It is also worth to note that at all NaI concentrations, the amount of dissociated Na$^+$ ions from NaI in hexanoyl chitosan electrolyte system is higher than lauroyl chitosan electrolyte. The obtained spectroscopic data were correlated with the conductivity performance in the following section.

Conductivity performance of hexanoyl chitosan and lauroyl chitosan

Figure 6 depicts the conductivity behaviors for hexanoyl chitosan and lauroyl chitosan electrolyte systems. Generally, at all salt concentrations, hexanoyl chitosan

Table 3 The values of ε_r, Q_2, τ_2, D, μ, and n obtained from the impedance spectroscopy method for hexanoyl chitosan-30 wt% NaI and lauroyl chitosan-30 wt% NaI

Electrolyte system	σ (S cm^{-1})	ε_r (at 400 kHz)	Q_2 (F^{-1})	τ_2 (s)	D (cm^2 s^{-1})	μ (cm^2 V^{-1} s^{-1})	n (cm^{-3})
Hexanoyl chitosan-30 wt% NaI	1.3×10^{-6}	216	3.0×10^{-6}	2.6×10^{-4}	5.9×10^{-9}	2.3×10^{-7}	3.6×10^{19}
Lauroyl chitosan-30 wt% NaI	1.1×10^{-8}	132	1.8×10^{-6}	3.2×10^{-3}	4.9×10^{-10}	1.9×10^{-8}	3.6×10^{18}
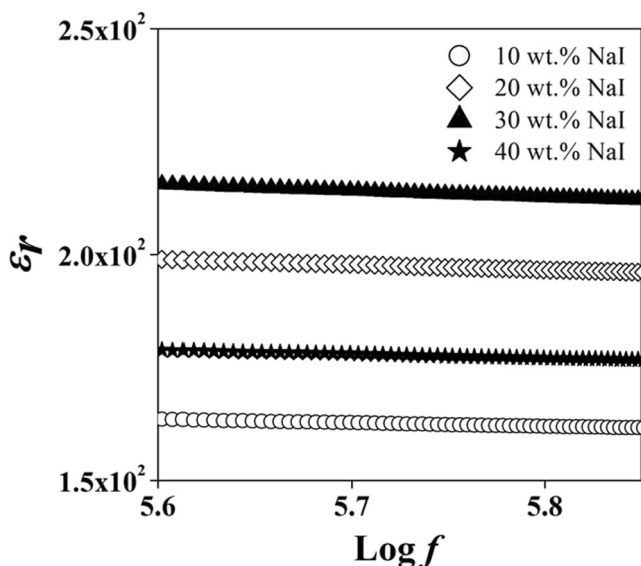
Fig. 10 Room temperature ε_r vs. log f plot for salted hexanoyl chitosan systems

Fig. 11 XRD diffractogram of hexanoyl chitosan containing *a* 0 wt%, *b* 10 wt%, *c* 20 wt%, *d* 30 wt%, and *e* 40 wt% of NaI

shows higher conductivity than lauroyl chitosan. The maximum conductivity achieved for hexanoyl chitosan and lauroyl chitosan is 1.3×10^{-6} and 1.1×10^{-8} S cm^{-1}, respectively. Both hexanoyl and lauroyl chitosan achieved the maximum conductivity at 30 wt% of NaI. The variation of conductivity as a function of NaI concentration in Fig. 6 is in close agreement with the variation of the intensity of $\nu(O{=}C{-}NHR)$ in Fig. 5. This suggested that higher conductivity is due to the increase in the number of dissociated Na$^+$ ions from Na$^+$ I$^-$ salt.

The molecular weights, M_w, of hexanoyl chitosan and lauroyl chitosan is 8.7×10^5 and 3.0×10^6 g mol^{-1}, respectively, estimated using GPC as described earlier in the "Experimental" section. The viscosity of an electrolyte depends upon the molecular weight of the polymer used [20]. Electrolyte viscosity, η, affects the ion mobility μ in accordance with Eq. (14) [21] where e is the electronic charge and r is the ionic radius. Thus, polymers with different molecular weights affect the conductivity behavior of electrolytes.

$$\eta = \frac{e}{6\pi r \mu} \qquad (14)$$

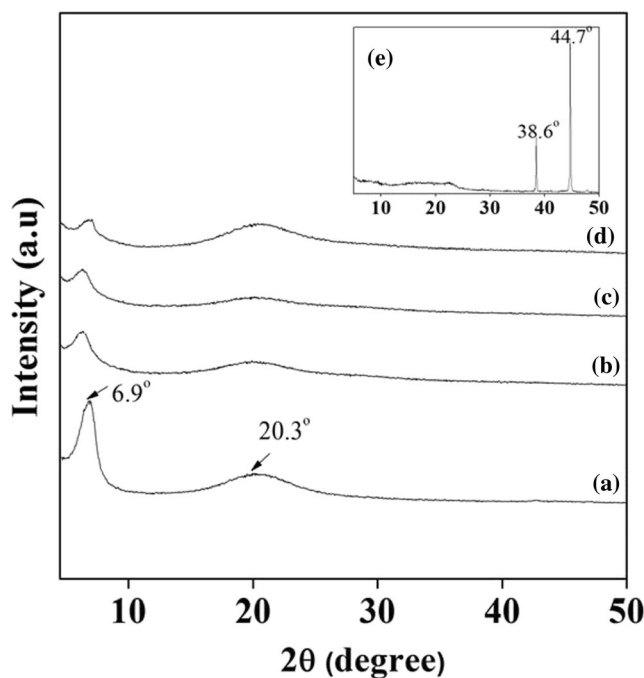Kumar and coworkers [22] have prepared poly(methyl methacrylate) (PMMA)-based electrolytes with three different molecular weights of PMMA. They reported that PMMA with lower M_w exhibited lower electrolyte viscosity and hence higher conductivity. Similarly, hexanoyl chitosan with lower molecular weight exhibited higher conductivity than lauroyl chitosan.

Motion of ion is also greatly affected by the flexibility of a polymer chain. The easy movement of a polymer chain increases the free volume, which facilitates the ion motion. Flexibility of a polymer chain can be reflected in the value of T_g of a polymer. Hexanoyl chitosan exhibited the lower value of T_g as compared to lauroyl chitosan (see Fig. 4). Thus, a more rapid segmental motion of hexanoyl chitosan polymer leads to higher ion mobility and results in a higher conductivity. The thermal results showed that higher conductivity in hexanoyl chitosan is due to higher ionic mobility.

The ionic mobility, μ, can be determined quantitatively by transient ionic current (TIC) measurement [23], nuclear magnetic resonance (NMR) spectroscopy [24], and impedance spectroscopy (IS) [17, 18]. In this work, the ionic mobility was calculated using impedance spectroscopy. Figure 7 shows the room

Table 4 The values of ε_r, Q_2, τ_2, D, μ, and n obtained from the impedance spectroscopy method for salted hexanoyl chitosan electrolyte system

NaI content (wt%)	σ (S cm^{-1})	ε_r (at 400 kHz)	Q_2 (F^{-1})	τ_2 (s)	D (cm^2 s^{-1})	μ (cm^2 V^{-1} s^{-1})	n (cm^{-3})
10	6.6×10^{-9}	164	2.0×10^{-6}	2.5×10^{-3}	8.1×10^{-10}	3.1×10^{-8}	1.3×10^{18}
20	8.0×10^{-7}	199	1.7×10^{-6}	1.1×10^{-3}	3.9×10^{-9}	1.5×10^{-7}	3.3×10^{19}
30	1.3×10^{-6}	216	3.0×10^{-6}	2.6×10^{-4}	5.9×10^{-9}	2.3×10^{-7}	3.6×10^{19}
40	1.8×10^{-8}	179	1.9×10^{-6}	1.3×10^{-3}	2.1×10^{-9}	8.2×10^{-8}	1.4×10^{18}

Fig. 12 Deconvoluted XRD diffractogram of hexanoyl chitosan containing *a* 0 wt%, *b* 10 wt%, *c* 20 wt%, *d* 30 wt%, and *e* 40 wt% of NaI
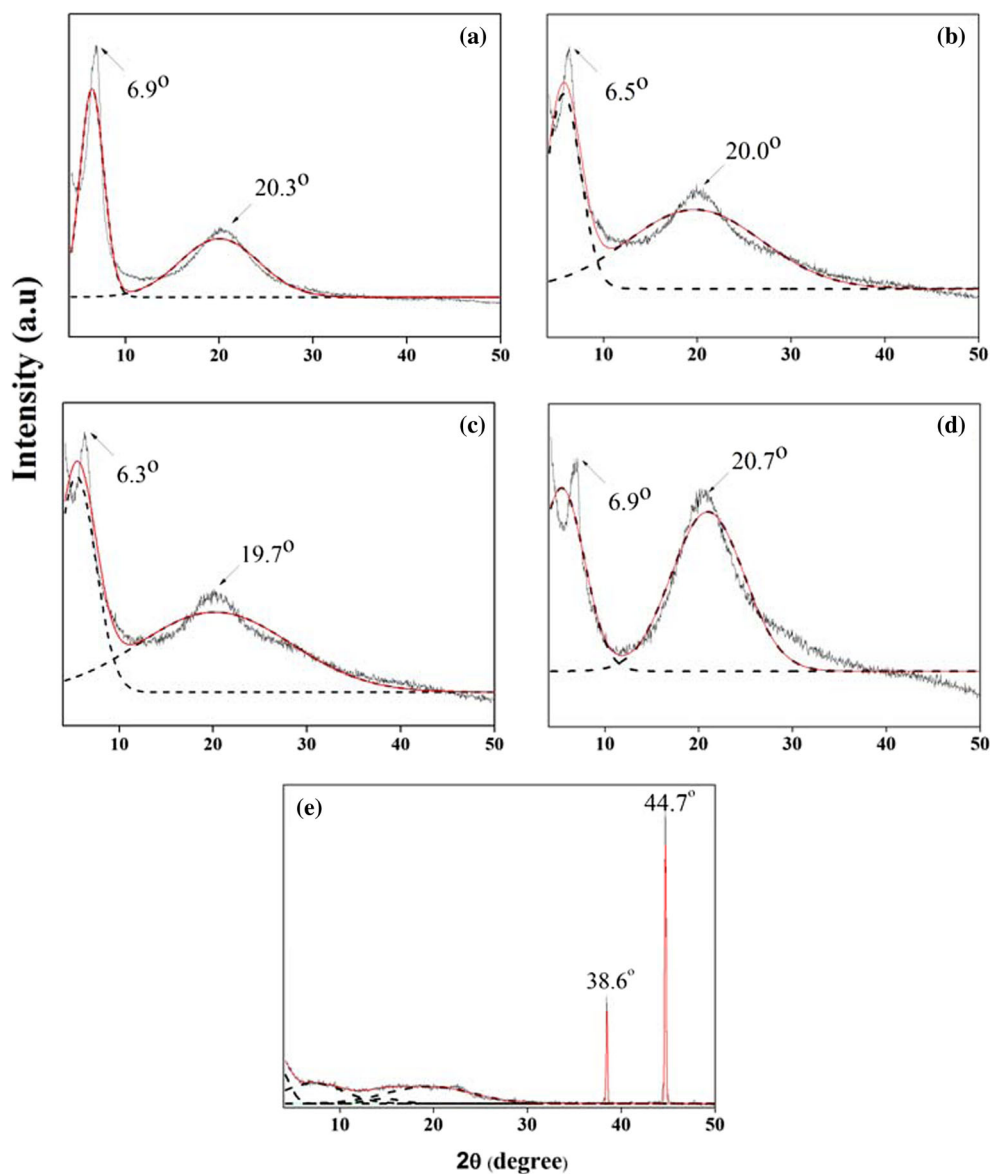
temperature complex impedance plot for hexanoyl chitosan with 30 wt% of NaI as a representative example. Equations (9) and (10) were used to fit the plots.

The value of diffusion coefficient, D, can be calculated if the values of τ_2, ε_r, and Q_2 are known according to Eq. (11). The value of τ_2 was taken at the frequency at Z_i in the vicinity of zero as shown in Fig. 2. The value of Q_2 was obtained by fitting the complex impedance plot. The value for ε_r was extracted from the plot of log ε_r vs. frequency as depicted in Fig. 8. The obtained values of τ_2, ε_r, and Q_2 and the calculated values of D were tabulated in Table 3. The obtained values of D were then used to calculate mobility, μ, and number, n, of free ions, using Eqs. (12) and (13), respectively. Results in Table 3 show quantitatively that the higher conductivity achieved by hexanoyl chitosan as compared to lauroyl

chitosan electrolyte system is attributed to the higher mobility of charge carriers.

Number of charge carriers, n, is another factor that governs the conductivity performance. From Table 3, the n for

Table 5 Degree of crystallinity for hexanoyl chitosan at various concentrations of NaI

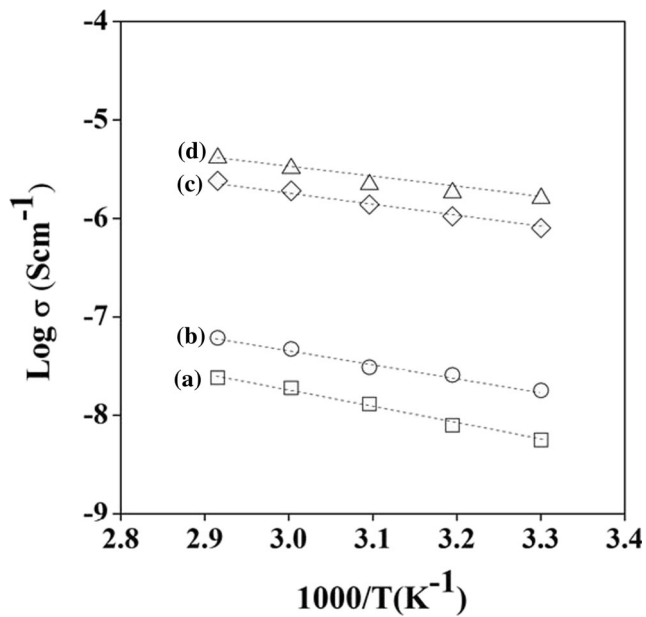| NaI content (wt%)	I_T (a.u.)	I_C (a.u.)	X_C (%)
0	33,227	15,586	46.9
10	34,381	11,006	32.0
20	22,882	7312	31.9
30	31,998	9835	30.1
40	27,444	15,542	36.6

Fig. 13 Temperature dependence conductivity of hexanoyl chitosan containing *a* 5 wt%, *b* 10 wt%, *c* 20 wt%, and *d* 30 wt% of NaI

hexanoyl chitosan electrolyte system is higher than lauroyl chitosan. The dielectric constants of neat hexanoyl chitosan and lauroyl chitosan polymer at 400 kHz are 2.7 and 1.9, respectively, as shown in Fig. 9. Higher dielectric constant of hexanoyl chitosan helps in greater dissociation of NaI salt
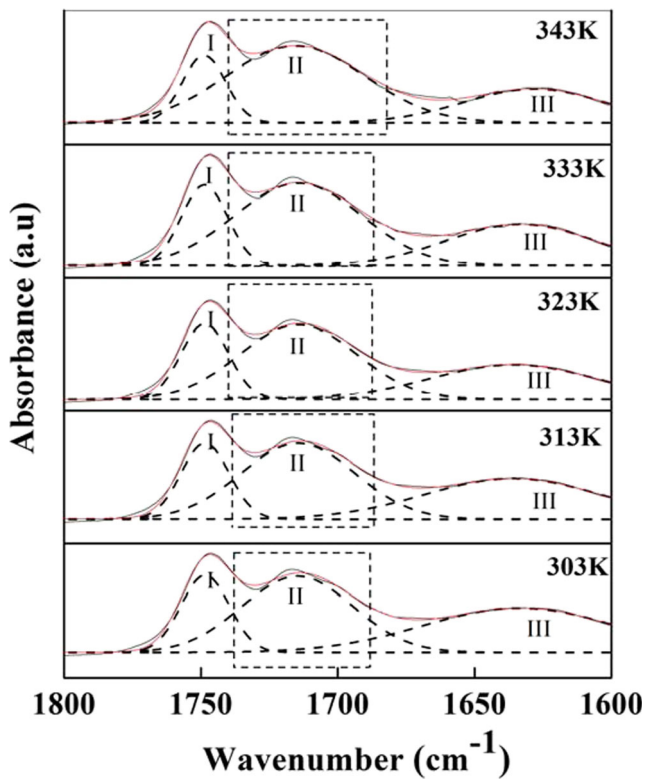

Fig. 14 Band fitting of IR spectra between 1600 and 1800 cm⁻¹ for hexanoyl chitosan-20 wt% NaI in temperature range of 303-343 K

and yields greater number of *n* which leads to greater conductivity.

Effect of salt concentration

Effect of NaI concentration on the transport properties of polymer electrolytes can be further evaluated using impedance spectroscopy. Figure 10 depicts the plots of room temperature ε_r vs. frequency for hexanoyl chitosan electrolyte system with different NaI concentrations.

The room temperature conductivity for hexanoyl chitosan electrolyte containing different concentrations of NaI differs as follows: σ (10 wt% NaI) < σ (40 wt%) < σ (20 wt%) < σ (30 wt%). This conductivity variation is in agreement with the variation of ε_r as shown in Fig. 10 where ε_r (10 wt% NaI) < ε_r (40 wt%) < ε_r (20 wt%) < ε_r (30 wt%). We had deduced that dielectric constant, ε_r, is a measure of stored ionic charge [25]. The higher value of ε_r represents higher number of ionic charge. NaI dissociates to give free Na⁺ cations and I⁻ anions. The variation in conductivity as a function of NaI content is due to the variation in the number of available free Na⁺ cations and I⁻ anions.

The initial increase of conductivity with increasing NaI content is due to the increase in the number of free ions. In order to analyze quantitatively the conductivity trend observed in Fig. 6a (as a representative example), μ and *n* of free ions were calculated using impedance spectroscopy with details discussed earlier. Table 4 lists the transport parameters, *D*, μ, and *n*, for hexanoyl chitosan electrolyte with various NaI contents.

It is apparent from the table that the increase of conductivity with increasing NaI concentration from 10 to 30 wt% is due to the increment in the number and mobility of free ions. Dissociation of NaI in the hexanoyl chitosan polymer matrix provides free ions for ionic conduction. More free ions dissociate from NaI with increment in the amount of NaI added. This led to conductivity enhancement.

However, beyond the optimum NaI content, strong coulombic attraction between the solvated salt ions resulted in the formation of ion pairs, triple ions, and even multiple ion aggregates. Increase of these neutral ion pairs or multiples led to a decline in the number of free ions and increase of medium viscosity. Higher viscosity of the medium reduced the mobility of ions. Consequently, the conductivity beyond 30 wt% NaI is reduced.

The XRD results shown in Fig. 11 reveal the variation in conductivity from the structural aspect. The diffractograms of the present electrolyte system were characterized by a sharp crystalline peak in the small-angle regime at $2\theta = 6.9°$ and an amorphous halo in the wide-angle regime.

Table 6 The values of ε_r, Q_2, τ_2, D, μ, and n for hexanoyl chitosan-20 wt% NaI as a function of temperature

Electrolyte system	σ (S cm^{-1})	ε_r (at 400 kHz)	Q_2 (F^{-1})	τ_2 (s)	D (cm^2 s^{-1})	μ (cm^2 V^{-1} s^{-1})	n (cm^{-3})
303	8.0×10^{-7}	199	1.7×10^{-6}	1.1×10^{-3}	3.9×10^{-9}	1.5×10^{-7}	3.3×10^{19}
313	1.9×10^{-6}	211	1.6×10^{-6}	1.1×10^{-3}	5.0×10^{-9}	1.8×10^{-7}	6.3×10^{19}
323	2.9×10^{-6}	228	1.9×10^{-6}	7.9×10^{-4}	5.5×10^{-9}	2.1×10^{-7}	7.2×10^{19}
333	3.1×10^{-6}	238	1.5×10^{-6}	1.1×10^{-3}	7.2×10^{-9}	2.6×10^{-7}	7.4×10^{19}
343	3.5×10^{-6}	259	1.9×10^{-6}	6.4×10^{-4}	8.8×10^{-9}	3.0×10^{-7}	7.5×10^{19}

From Fig. 11, the relative intensity of the crystalline peak at $2\theta = 6.9°$ was found to decrease with increasing NaI content. This suggests that the crystallinity of hexanoyl chitosan had changed in the presence of NaI salt. In order to quantify the crystallinity of the electrolyte, the diffractograms shown in Fig. 11 were deconvoluted. Figure 12 shows the deconvoluted diffractogram for hexanoyl chitosan-NaI electrolyte system. The degree of crystallinity, X_C, was then calculated using the equation

$$Xc = \frac{I_C}{I_T} \times 100\% \qquad (15)$$

where I_C is the area under the sharp crystalline peaks at $2\theta = 6.9°$ and I_T is the total area under the diffractogram from $2\theta = 5°$ to $50°$. Values of I_C and I_T obtained by deconvolution of XRD diffractogram are tabulated in Table 5. The degree of crystallinity was then calculated from the known value of I_C and I_T.

From Table 5, the degree of crystallinity for neat hexanoyl chitosan is 46.9%. Upon addition of 10 wt% NaI, the degree of crystallinity decreases to 32.0% and reaches the lowest value of 30.1% for sample with 30 wt% NaI. The decrease of crystallinity of hexanoyl chitosan upon addition of salt may be attributed to the breaking of the order of hexanoyl chitosan by NaI. Neat hexanoyl chitosan has a layered structure, where the main chains with polysaccharide rings form layers separated by hydrocarbon side chains [8]. The main polysaccharide chains are not all coplanar and have different rotation angles relative to each other due to the ether linkage. However, the rotational freedom of main chains is constrained under hydrogen bonds in chitosan structure, maintaining the ordered phases of hexanoyl chitosan. After addition of NaI, some hydrogen bonds may be broken to surround the salt ions causing destruction of ordered phases which decreases the crystallinity of hexanoyl chitosan. The decrease in crystallinity or increase in amorphousness is in agreement with the increment of conductivity. Rapid segmental motion of polymer chain takes place in amorphous region. A more rapid polymer segmental motion increases the mobility of ions that leads to higher ionic conductivity. Sample containing 30 wt% NaI exhibited the lowest crystallinity structure and hence the highest conductivity. Addition of 40 wt% NaI has resulted in an increase in crystallinity due to the existence of additional crystalline peaks at $2\theta = 38.6°$ and $44.7°$ as shown in Fig. 11.

Effect of temperature

Temperature is another factor that governs the conductivity performance of a polymer electrolyte. The plots of ionic conductivity of hexanoyl chitosan-NaI system against reciprocal temperature are presented in Fig. 13. It is shown that conductivity increases with increasing temperature. In the temperature range investigated, hexanoyl chitosan containing 30 wt% of NaI exhibits the highest conductivity. The effect of temperature on the transport properties was further evaluated using impedance spectroscopy. Table 6 lists the transport properties for hexanoyl chitosan containing 20 wt% NaI as a representative example in the temperature range of 303 to 343 K.
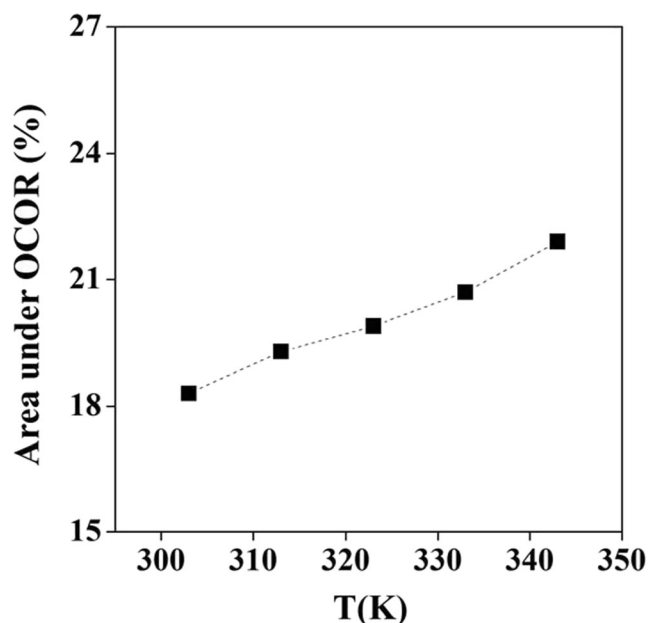

Fig. 15 The calculated area under OCOR peak for hexanoyl chitosan-20 wt% NaI in temperature range 303–343 K

The polymer-Na^+ interactions are electrostatic in nature. A Na^+ cation can hop from one complexation site to another leaving a vacancy which will be filled by another Na^+ from a neighboring site. As temperature increases, more Na^+ cations acquire sufficient kinetic energy from its environment to hop to the next complexation site, an increment in the migration of Na^+ cations, μ. In addition, Na^+ cations with sufficient energy can also break its ionic bond with I^- anion. This increases NaI dissociation and redissociation of ion pairs and ion aggregates, which yields greater number of ions, n, for conduction.

The increment of n with temperature is further supported by spectroscopic data. Similar to the O=C-NHR band, the OCOR band can also be used to indicate the amount of Na^+ ions that have complexed with the oxygen atom in OCOR functional group, i.e., the amount of dissociated Na^+ ions from NaI. The peak of OCOR was deconvoluted as a function of temperature (see Fig. 14, region II), and the deconvolution results are presented in Fig. 15. In Fig. 15, it is observed that the amount of dissociated Na^+ ions increases with temperature. This is in agreement with the n calculated from impedance spectroscopy as listed in Table 6.

Conclusions

Both FTIR and DSC studies showed that NaI interacted with hexanoyl chitosan and lauroyl chitosan. Hexanoyl chitosan exhibited better conductivity performance than lauroyl chitosan. DSC results showed that higher conductivity in hexanoyl chitosan was due to higher ionic mobility. Hexanoyl chitosan has higher dielectric value than lauroyl chitosan. This resulted in greater salt dissociation by hexanoyl chitosan and hence greater number of ionic species for conduction. Greater number of ions in hexanoyl chitosan system was supported by spectroscopic and impedance results. XRD results showed the influence of NaI on the crystalline content of the prepared electrolyte system. Conductivity is found to increase with decrement in the degree of crystallinity. The effects of salt concentration and temperature on the conductivity were understood on the basis of the number and mobility of ions. These parameters were calculated using impedance spectroscopy.

References

1. Alves R, Donoso JP, Magon CJ, Silva IDA, Pawlicka A, Silva MM (2015) Solid polymer electrolytes based on chitosan and europium triflate. J Non-Cryst Solids 432 part B: 307–312
2. Rudhziah S, Ahmad A, Ahmad I, Mohamed NS (2015) Biopolymer electrolytes based on blend of kappa-carrageenan and cellulose derivatives for potential application in dye sensitized solar cell. Electrochim Acta 175:162–168
3. Majid SR, Sabadini RC, Kanicki J, Pawlicka A (2014) Impedance analysis of gellan gum-poly(vinyl pyrrolidone) membranes. Mol Cryst Liq Cryst 604:84–95
4. Woo HJ, Majid SR, Arof AK (2012) Dielectric properties and morphology of polymer electrolyte based on poly(ε-caprolactone) and ammonium thiocyanate. Mater Chem Phys 134:755–761
5. Aziz SB, Abidin ZHZ (2014) Electrical and morphological analysis of chitosan:AgTf solid electrolyte. Mater Chem Phys 144:280–286
6. Winie T, Majid SR, Khiar ASA, Arof AK (2006) Ionic conductivity of chitosan membrane and application for electrochemical devices. Polym Adv Technol 17:523–527
7. Moore G, Goerge A (1981) Reactions of chitosan: 2. Preparation and reactivity of N-acyl derivatives of chitosan. Int J Biol Micromol 3:292–296
8. Zong Z, Kimura Y, Takahashi M, Yamane H (2000) Characterization of chemical and solid state structures of acylated chitosans. Polymer 41:899–906
9. Nishimura S, Kohgo O, Kurita K, Kuzuhara H (1991) Chemospecific manipulations of a rigid polysaccharide: syntheses of novel chitosan derivatives with excellent solubility in common organic solvents by regioselective chemical modifications. Macromolecules 24:4745–4748
10. Yalpani M, Hall LD (1984) Some chemical and analytical aspects of polysaccharide modifications. III. Formation of branched-chain, soluble chitosan derivatives. Macromolecules 17:272–281
11. Winie T, Arof AK (2006) Hexanoyl chitosan-based gel electrolyte for use in lithium-ion cell. Polym Adv Technol 17:552–555
12. Rosli NHA, Chan CH, Subban RHY, Winie T (2012) Studies on the structural and electrical properties of hexanoyl chitosan/polystyrene-based polymer electrolytes. Phys Procedia 25:215–220
13. Winie T, Shahril NSM, Chan CH, Arof AK (2014) Selective localization of lithium trifluoromethanesulfonate in the blend of hexanoyl chitosan and polystyrene. High Perform Polym 26:666–671
14. Winie T, Shahril NSM (2015) Conductivity enhancement by controlled percolation of inorganic salt in multiphase hexanoyl chitosan/polystyrene polymer blends. Front Mater Sci 9:132–140
15. Winie T, Rosli NHA, Ahmad MR, Subban RHY, Chan CH (2012) TiO_2 dispersed hexanoyl chitosan-polystyrene- $LiCF_3SO_3$ composite electrolyte characterized for electrical and tensile properties. Polym Res J 7:171–181
16. Winie T, Arof AK (2014) Impedance spectroscopy: basic concepts and application for electrical evaluation of polymer electrolytes. In: Impedance Spectroscopy, 1st edn. Apple Academic Press, USA, pp 335–363
17. Linford RG (1988) In: Chowdari BVR, Radhakrishna S (eds) Solid state Ionics devices. World Scientific, Singapore, pp 551–571
18. Arof AK, Amirudin S, Yusof SZ, Noor IM (2014) A method based on impedance spectroscopy to determine transport properties of polymer electrolytes. R Soc Chem 16:1856–1867
19. Sim LN, Majid SR, Arof AK (2012) FTIR studies of PEMA/PVdF-HFP blend polymer electrolyte system incorporated with $LiCF_3SO_3$ salt. Vib Spectrosc 58:57–66

20. Sharma JP, Sekhon SS (2006) PMMA-based polymer gel electrolytes containing NH$_4$PF$_6$: role of molecular weight of polymer. Mater Sci Eng B 129:104–108

21. Bohnke O, Frand G, Resrazi M, Rousseelet C, Truche C (1993) Fast ion transport in new lithium electrolytes gel with PMMA. Influence of polymer concentration. Solid State Ionics 66:97

22. Kumar R, Sekhon SS (2008) Effect of molecular weight of PMMA on the conductivity and viscosity behavior of polymer gel electrolytes containing. Ionics 14:509–514

23. Chandra S, Tolpadi SK, Hashmi SA (1988) Transient ionic current measurement of ionic mobilities in a few proton conductors. Solid State Ionics 28–30:651–655

24. Williamson MJ, Southhall JP, Hubbard VSA (1998) NMR measurements of ionic mobility in model polymer electrolyte solutions. Electrochim Acta 43:1415–1420

25. Winie T, Arof AK (2004) Dielectric behaviour and AC conductivity of LiCF$_3$SO$_3$ doped H-chitosan polymer films. Ionics 10:193–199